

Metabolic and energy correlates of intracellular pH in progressive fatigue of squid (*L. brevis*) mantle muscle

H. O. PÖRTNER, E. FINKE, AND P. G. LEE

Alfred-Wegener-Institut für Polar- und Meeresforschung, Biologie I/Ökophysiologie,
D-27515 Bremerhaven, Germany; and Marine Biomedical Institute,
University of Texas Medical Branch, Galveston, Texas 77550

Pörtner, H. O., E. Finke, and P. G. Lee. Metabolic and energy correlates of intracellular pH in progressive fatigue of squid (*L. brevis*) mantle muscle. *Am. J. Physiol.* 271 (*Regulatory Integrative Comp. Physiol.* 40): R1403–R1414, 1996.—Squid (*Lolliguncula brevis*) were exercised at increasing swimming speeds to allow us to analyze the correlated changes in intracellular metabolic, acid-base, and energy status of the mantle musculature. Beyond a critical swimming velocity of 1.5 mantle lengths/s, an intracellular acidosis developed that was caused by an initial base loss from the cells, the onset of respiratory acidification, and, predominantly, octopine formation. The acidosis was correlated with decreasing levels of phospho-L-arginine and, thus, supported ATP buffering at the expense of the phosphagen. Monohydrogenphosphate, the actual substrate of glycogen phosphorylase, accumulated, enabling glycogen degradation, despite progressive acidosis. In addition to octopine, succinate, and α -glycerophosphate accumulation, the onset of acidosis characterizes the critical velocity and indicates the transition to a non-steady-state time-limited situation. Accordingly, swimming above the critical velocity caused cellular energy levels (in vivo Gibbs free energy change of ATP hydrolysis) to fall. A minimal value was reached at about -45 kJ/mol. Model calculations demonstrate that changes in free Mg^{2+} levels only minimally affect ATP free energy, but minimum levels are relevant in maintaining functional concentrations of Mg^{2+} -complexed adenylates. Model calculations also reveal that phosphagen breakdown enabled *L. brevis* to reach swimming speeds about three times higher than the critical velocity. Comparison of two offshore squid species (*Loligo pealei* and *Illex illecebrosus*) with the estuarine squid *L. brevis* indicates that the latter uses a strategy to delay the exploitation of high-energy phosphates and protect energy levels at higher than the minimum levels (-42 kJ/mol) characterizing fatigue in the other species. A more economical use of anaerobic resources and an early reduction in performance may enable *L. brevis* to tolerate more extreme environmental conditions in shallow estuarine waters and even hypoxic environments and to prevent a fatal depletion of energy stores.

acidosis; arginine kinase; ATP buffering; brief squid; free magnesium; Gibbs free energy change of ATP hydrolysis; glycogen phosphorylase; *Lolliguncula brevis*; mantle muscle fatigue; myokinase; octopine; phosphagen; phospho-L-arginine; swimming velocity

AS A SPECIES ADAPTED to waters of variable salinity, the brief squid *Lolliguncula brevis* is able to enter shallow waters of inshore and estuarine environments. It has also been reported to enter hypoxic bottom waters formed when low-salinity water masses lie on top of high-salinity water layers, preventing convective gas exchange between the bottom layer and the air (37). As a coastal and inshore species, *L. brevis* will usually not

swim long distances. It is characterized by a smaller body size, a feature possibly also related to its life in shallow waters, than the larger squid living farther offshore and on the shelf (e.g., *Loligo pealei* and *Illex illecebrosus*). The fins are well developed, but less than in other loliginids, e.g., *L. pealei* or *Loligo forbesi* (11, 39).

In comparison to most other squid species, the brief squid appears rather tolerant of fluctuations in environmental parameters. Nonetheless, it has to cope with the evolutionary constraints of all cephalopods, i.e., jet propulsion as an energetically inefficient mode of locomotion, a low oxygen capacity of the blood, and an extracellular blood pigment, hemocyanin. In a study of basic metabolic changes during increased swimming speeds, we demonstrated that a critical swimming speed exists that is determined by oxygen availability to the mantle tissue (11). Insufficient oxygen supply to mantle mitochondria elicits the onset of anaerobic energy production in the cytosol and the mitochondria. This finding is quite opposite to the situation in many other vertebrate and invertebrate species, where energy requirements in excess of aerobic energy production are covered by anaerobic metabolism in the cytosol, with mitochondria remaining aerobic. Mitochondrial hypoxia causes the critical speed of *L. brevis* to be relatively low compared with that of pelagic fish of similar size. This finding is attributed to the life of these squid in shallow coastal and bay waters, limiting the necessity to maintain high swimming speeds. Although net use of anaerobic resources is observed, the mode of metabolism maintained during fast swimming is also described by an oscillation between periods of high-anaerobic and low-aerobic muscular activity, extending the time period during which anaerobic resources can be exploited (11).

Previously, we reported the activity levels and the associated rate and mode of metabolism in freely swimming unrestrained *L. brevis* at different swimming speeds (11). The present study was designed 1) to extend our insight into the progressive development of non-steady-state changes in metabolism and energy status above the critical swimming velocity, 2) to quantify which biochemical mechanisms are used to coordinate the net use of different anaerobic resources, and 3) to identify the mechanisms that extend the period of anaerobic exercise. Finally, we propose a quantitative model of phosphagen utilization that also considers the coordination between the developing acidosis and the exploitation of high-energy phosphates. These processes are crucial in maintaining the energy

Metabolic and energy correlates of intracellular pH in progressive fatigue of squid (*L. brevis*) mantle muscle

H. O. PÖRTNER, E. FINKE, AND P. G. LEE

Alfred-Wegener-Institut für Polar- und Meeresforschung, Biologie I/Ökophysiologie,
D-27515 Bremerhaven, Germany; and Marine Biomedical Institute,
University of Texas Medical Branch, Galveston, Texas 77550

Pörtner, H. O., E. Finke, and P. G. Lee. Metabolic and energy correlates of intracellular pH in progressive fatigue of squid (*L. brevis*) mantle muscle. *Am. J. Physiol.* 271 (*Regulatory Integrative Comp. Physiol.* 40): R1403–R1414, 1996.—Squid (*Lolliguncula brevis*) were exercised at increasing swimming speeds to allow us to analyze the correlated changes in intracellular metabolic, acid-base, and energy status of the mantle musculature. Beyond a critical swimming velocity of 1.5 mantle lengths/s, an intracellular acidosis developed that was caused by an initial base loss from the cells, the onset of respiratory acidification, and, predominantly, octopine formation. The acidosis was correlated with decreasing levels of phospho-L-arginine and, thus, supported ATP buffering at the expense of the phosphagen. Monohydrogenphosphate, the actual substrate of glycogen phosphorylase, accumulated, enabling glycogen degradation, despite progressive acidosis. In addition to octopine, succinate, and α -glycerophosphate accumulation, the onset of acidosis characterizes the critical velocity and indicates the transition to a non-steady-state time-limited situation. Accordingly, swimming above the critical velocity caused cellular energy levels (in vivo Gibbs free energy change of ATP hydrolysis) to fall. A minimal value was reached at about -45 kJ/mol. Model calculations demonstrate that changes in free Mg^{2+} levels only minimally affect ATP free energy, but minimum levels are relevant in maintaining functional concentrations of Mg^{2+} -complexed adenylates. Model calculations also reveal that phosphagen breakdown enabled *L. brevis* to reach swimming speeds about three times higher than the critical velocity. Comparison of two offshore squid species (*Loligo pealei* and *Illex illecebrosus*) with the estuarine squid *L. brevis* indicates that the latter uses a strategy to delay the exploitation of high-energy phosphates and protect energy levels at higher than the minimum levels (-42 kJ/mol) characterizing fatigue in the other species. A more economical use of anaerobic resources and an early reduction in performance may enable *L. brevis* to tolerate more extreme environmental conditions in shallow estuarine waters and even hypoxic environments and to prevent a fatal depletion of energy stores.

acidosis; arginine kinase; ATP buffering; brief squid; free magnesium; Gibbs free energy change of ATP hydrolysis; glycogen phosphorylase; *Lolliguncula brevis*; mantle muscle fatigue; myokinase; octopine; phosphagen; phospho-L-arginine; swimming velocity

AS A SPECIES ADAPTED to waters of variable salinity, the brief squid *Lolliguncula brevis* is able to enter shallow waters of inshore and estuarine environments. It has also been reported to enter hypoxic bottom waters formed when low-salinity water masses lie on top of high-salinity water layers, preventing convective gas exchange between the bottom layer and the air (37). As a coastal and inshore species, *L. brevis* will usually not

swim long distances. It is characterized by a smaller body size, a feature possibly also related to its life in shallow waters, than the larger squid living farther offshore and on the shelf (e.g., *Loligo pealei* and *Illex illecebrosus*). The fins are well developed, but less than in other loliginids, e.g., *L. pealei* or *Loligo forbesi* (11, 39).

In comparison to most other squid species, the brief squid appears rather tolerant of fluctuations in environmental parameters. Nonetheless, it has to cope with the evolutionary constraints of all cephalopods, i.e., jet propulsion as an energetically inefficient mode of locomotion, a low oxygen capacity of the blood, and an extracellular blood pigment, hemocyanin. In a study of basic metabolic changes during increased swimming speeds, we demonstrated that a critical swimming speed exists that is determined by oxygen availability to the mantle tissue (11). Insufficient oxygen supply to mantle mitochondria elicits the onset of anaerobic energy production in the cytosol and the mitochondria. This finding is quite opposite to the situation in many other vertebrate and invertebrate species, where energy requirements in excess of aerobic energy production are covered by anaerobic metabolism in the cytosol, with mitochondria remaining aerobic. Mitochondrial hypoxia causes the critical speed of *L. brevis* to be relatively low compared with that of pelagic fish of similar size. This finding is attributed to the life of these squid in shallow coastal and bay waters, limiting the necessity to maintain high swimming speeds. Although net use of anaerobic resources is observed, the mode of metabolism maintained during fast swimming is also described by an oscillation between periods of high-anaerobic and low-aerobic muscular activity, extending the time period during which anaerobic resources can be exploited (11).

Previously, we reported the activity levels and the associated rate and mode of metabolism in freely swimming unrestrained *L. brevis* at different swimming speeds (11). The present study was designed 1) to extend our insight into the progressive development of non-steady-state changes in metabolism and energy status above the critical swimming velocity, 2) to quantify which biochemical mechanisms are used to coordinate the net use of different anaerobic resources, and 3) to identify the mechanisms that extend the period of anaerobic exercise. Finally, we propose a quantitative model of phosphagen utilization that also considers the coordination between the developing acidosis and the exploitation of high-energy phosphates. These processes are crucial in maintaining the energy

content of the ATP system until a limiting level may be reached.

MATERIALS AND METHODS

Animals. Common brief squid (*L. brevis*, Blainville, 1823, 6.6–34.2 g) were caught in April and May 1993 in the Galveston Ship Channel and Galveston Harbor by the fishermen of the Marine Biomedical Institute of the University of Texas (Galveston, TX) and kept in recirculating aquaria with natural seawater under conditions similar to those in the natural habitat (24–26‰ salinity, 20–22°C). The squid were allowed to adjust to the aquarium for ≥24 h. The animals were fed small fish and mysid shrimp, but not during the last 24 h before experimentation.

Experimental procedure. For the collection of control samples, each individual squid was placed into a darkened aquarium containing 4 liters of continuously aerated seawater (25 ± 1‰ salinity, 20 ± 1°C). After 60–100 min of recovery from handling, ethanol (120 ml) was added to the aquarium through tubing placed close to the aeration stone to ensure rapid and full mixing with the seawater. The final maximum concentration of the anesthetic was 3 ml/100 ml. Anesthesia was complete after 2–4 min, as indicated by the cessation of ventilatory activity.

Squid were exercised in a Brett-type respirometer (4), as described by Finke et al. (11). The respirometer contained 17.76 liters of normoxic seawater at 20 ± 1°C, with a removable animal chamber (10.2-cm tube diameter) placed in a bath of fresh aerated seawater of the same temperature. The animals were exercised in the open respirometer, such that the water remained fully saturated with air at all times. After 30 min of acclimatization at a water velocity of 3.0 cm/s, a stepwise increase in water velocity by 3.0 cm/s every 6 min led to various final swimming speeds. At the highest velocities, chosen to be slightly submaximum but still fatiguing, the onset of fatigue became obvious when the squid repeatedly touched the downstream grid of the swimming chamber with the tip of their arms or finally ceased swimming, indicating exhaustion. For a comparison of non-steady-state metabolic changes at different swimming speeds, the length of this period of maximum exercise was adopted as a basis for subsequent experiments, and further animals were exercised at lower water velocities for a total period of 39 ± 1 min (including the time required for the stepwise increase in water velocity). Swimming speeds were normalized in mantle lengths per second.

At the end of the exercise period, the animal chamber was separated from the rest of the system, and the experimental animals were rapidly transferred to seawater of the same temperature containing 1.5 or 3.0 ml/100 ml ethanol. Animals responding to this procedure by vigorous jets were removed from the analyses. Anesthesia was complete after 20 s–2 min, depending on the level of exercise.

Muscle samples were obtained using a parallel arrangement of scalpel blades (31). The tissue samples were freeze-clamped immediately, weighed briefly, wrapped in aluminum foil, and stored under liquid nitrogen until analyzed. Additionally, the residues of each specimen were weighed to determine the body weight of the whole animal, and the mantle length was measured.

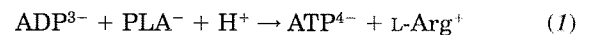
Analyses. All analyses were carried out at the Alfred Wegener Institute. With the use of tissue samples stored under liquid nitrogen, intracellular pH (pH_i) and tissue concentration of CO₂ were evaluated by the homogenate technique (29). Briefly, tissue samples were ground under liquid nitrogen with use of a porcelain mortar and pestle.

Care was taken during this procedure to minimize contamination of the muscle powder with condensing CO₂. In a closed Eppendorf tube, the powder was mixed with ice-cold medium (pH ~7) containing potassium fluoride (160 mmol/l) and the disodium salt of nitrilotriacetic acid (2.2 mmol/l; Sigma Chemical, St. Louis, MO). After brief centrifugation (5–15 s), pH and total CO₂ were measured (29). By use of the measured pH_i values and the appropriate values of apparent dissociation constant of carbonic acid and CO₂ solubility (16), intracellular PCO₂ was calculated for the mantle by use of a modified Henderson-Hasselbalch equation (29). For the potential errors in the estimate of PCO₂ values (use of homogenate-derived pH_i instead of a value derived from weak acid distribution; unequal CO₂ distribution between aerobic and anaerobic mantle muscle layers), the calculated PCO₂ values are considered to be close to those of the central part of squid mantle (31).

Respiratory and nonrespiratory changes in mantle acid-base status were analyzed with a pH-bicarbonate diagram. The nonbicarbonate buffer value of the tissue was estimated according to the procedure of Pörtner (26).

Samples of the tissue powder were also extracted in perchloric acid, as described earlier (11) for enzymatic analyses of several metabolites in the pH-neutralized extracts. P_i was estimated according to Pörtner (26). Octopine, phospho-L-arginine (PLA) and L-arginine (L-Arg) were determined according to Grieshaber et al. (14). ATP was assayed according to Bergmeyer et al. (3).

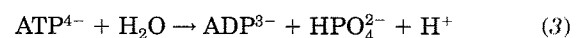
Calculations. The levels of free ADP and AMP (11) had been calculated on the basis of the equilibrium of arginine kinase (AK) and myokinase. Equilibrium constants for both enzymes (10, 36) were corrected for experimental temperature and pH dependence as related to changing proton and Mg²⁺ binding of the adenylates and the proton turnover of the AK reaction (27, 32). Briefly, an evaluation of the influence of Mg²⁺ levels and pH on apparent reaction equilibria requires the definition of reference reactions with a later consideration of how the fractional concentration of ionized species (e.g., f_{ADP³⁻}) depends on pH and Mg²⁺ levels. For the analysis of the pH dependence of AK, this reference reaction was



The reference reaction defined for the analysis of pH dependence of myokinase was



The reference reaction for an estimate of the free energy change of ATP hydrolysis was



The respective mass action constants derived from these reference equations are named K_1 , for example

$$K_{1\text{AK}} = [\text{ATP}^{4-}] \cdot [\text{L-Arg}^+] / [\text{ADP}^{3-}] \cdot [\text{PLA}^-] \cdot [\text{H}^+] \quad (4)$$

where [ATP⁴⁻], [L-Arg⁺], [ADP³⁻], [PLA⁻], and [H⁺] are ATP⁴⁻, L-Arg⁺, ADP³⁻, PLA⁻, and H⁺ concentration, respectively. K_1 is related to the apparent mass action constant K_{app} , which can be evaluated from the total metabolite concentrations (as measured in perchloric acid extracts). K_1 can be evaluated from K_{app} , for example, by use of the respective relationship between K_1 and K_{app} for AK as

$$K_{\text{appAK}} = [\text{ATP}]_{\text{tot}} \cdot [\text{L-Arg}]_{\text{tot}} / [\text{ADP}]_{\text{tot}} \cdot [\text{PLA}]_{\text{tot}} \cdot [\text{H}^+] \\ = K_{1\text{AK}} \cdot f_{\text{ADP}^{3-}} \cdot f_{\text{PLA}^-} / f_{\text{ATP}^{4-}} \quad (5)$$

where f represents the fractional levels of ionized species in the total concentration of a substance.

A version of K_{appAK} specific for a certain pH value is

$$K_{appAK}(pH) = K_{appAK}/[H^+] \quad (6)$$

(Total ADP in this context means total free ADP, i.e., the sum of free ADP species effectively "seen" by the AK in vivo; see below.)

Enzyme equilibria at 20°C were calculated using the van't Hoff equation by adopting a standard enthalpy (ΔH°) value of 1.5 kJ/mol for the reference reaction of myokinase (36) and a standard apparent (meaning at specified pH, free magnesium, temperature, pressure, and ionic strength) enthalpy value ($\Delta H'^\circ$) of -11.93 kJ/mol for K_{appAK} at pH 7.0 and 1 mM free Mg^{2+} with the assumption of identical values for arginine and creatine kinase (35). The value given by Teague and Dobson (35) is close to that reported by Woledge (40) for creatine kinase in phosphate buffer solution and differs from that found in carnosine buffer, which was more widely propagated (7, 40). The former value was used in the present study emphasizing that a solution containing potassium chloride and phosphate should closely mimic the cellular conditions for buffer and enzyme reactions (cf. Ref. 26). Our previous values (32) have been recalculated accordingly (Table 1). Fractional levels (f) of reaction partners as they varied with fluctuating Mg^{2+} levels and pH were calculated from the respective dissociation equilibria with use of constants of Mg^{2+} and H^+ binding as compiled earlier (2, 23, 30; for cellular potassium levels of 0.16 mol/l, if available, and for the respective ionic strength, cf. Ref. 13), for example

$$f_{PLA^-} = [PLA^-]/[PLA]_{tot} = \{1 + ([Mg^{2+}]/K_{dMgPLA}) + ([H^+]/K_{aHPLA})\}^{-1} \quad (7)$$

where K_a and K_d are acid and dissociation constants.

Calculations of the free energy change of ATP hydrolysis under in vivo conditions are now possible, starting with an evaluation of standard apparent equilibrium constant of this reaction (K'° ; concentrations of reactants are 1 mol/l for the sum of all species of a reactant) and determining the respective K_1 to be able to evaluate the influence of Mg^{2+} levels and pH on K'° (cf. Refs. 1 and 2)

$$K'^\circ = [ADP]_{tot} \cdot [P_i]_{tot} / [ATP]_{tot} = K_1 \cdot f_{ATP^{4-}} / [H^+] \cdot f_{ADP^{3-}} \cdot f_{P_i^{2-}} \quad (8)$$

$$\Delta G'^\circ = -RT \ln K'^\circ \quad (9)$$

where R is the gas constant, T is the absolute temperature (in K), $[P_i]$ is P_i concentration, and $\Delta G'^\circ$ is the standard apparent Gibbs free energy change.

The effective free energy change of ATP hydrolysis under in vivo conditions results when the actual in vivo concentrations of unbound (free) ATP, ADP, and P_i are evaluated

$$dG/d\xi = \Delta G'^\circ + RT \cdot \ln([ADP]_{free,tot} \cdot [P_i]_{free,tot} / [ATP]_{free,tot}) \quad (10)$$

All ATP, PLA, and L-Arg measured in perchloric acid extracts are believed to be unbound in the cell, whereas much of the ADP is bound to ATPases. Because only the free concentrations will be effective (cf. Ref. 38), the total (tot) concentration of unbound (free) ADP is evaluated from the equilibrium of AK

$$[ADP]_{free,tot} = [ATP]_{free,tot} \cdot [L-Arg]_{free,tot} / [PLA]_{free,tot} \cdot K_{appAK} \cdot [H^+] \quad (11)$$

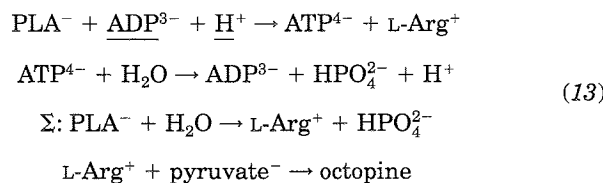
The term $[P_i]_{tot}$ needs special consideration, because perchloric acid extraction tends to overestimate the concentration of free P_i , a phenomenon typical for tissues containing a significant amount of mitochondria. It needs to be emphasized that (with the adequate experimental precautions) this finding is most likely not to be caused by the hydrolysis of organic phosphates during tissue sampling and extraction (see RESULTS). Therefore, the measured phosphate values were corrected to average control values of $\sim 1 \mu\text{mol/g}$ wet wt in accordance with measurements by noninvasive ^{31}P nuclear magnetic resonance (NMR) in the mantle of resting *L. brevis* (H. O. Pörtner, D. M. Webber, P. G. Lee, R. K. O'Dor, and M. Quast, unpublished observations).

The effective Gibbs free energy change can now be calculated from the equation of AK by substituting the term $[ADP]_{free,tot}$ in Eq. 10 with Eq. 11

$$dG/d\xi = \Delta G'^\circ + RT \cdot \ln([L-Arg]_{free,tot} \cdot [P_i]_{free,tot} / [PLA]_{free,tot} \cdot [H^+] \cdot K_{appAK}) \quad (12)$$

Calculations were performed assuming levels of free intracellular Mg^{2+} of 1 mmol/l (cf. Refs. 9 and 23). A potential change in free intracellular Mg^{2+} levels was considered in its influence on the levels of ATP free energy changes.

Our previous (32) and the present analysis suggest that values of ATP free energy do not fall below a low threshold value during fatigue. The importance of the phosphagen system in maintaining ATP free energy at an elevated level, thereby extending the period of anaerobic exercise, was illustrated by determining the swimming speed that is reached with and without transphosphorylation of PLA. To this end, the specific effect of each individual parameter influencing AK (pH_i and contents of octopine or free ADP) was evaluated assuming constant values for the remaining two parameters (see Fig. 6). Briefly, PLA transphosphorylation is elicited by an accumulation of ADP and H^+ . P_i is released via ATP hydrolysis. L-Arg is removed from the AK reaction by octopine formation, thereby causing maintenance of a higher ATP-to-ADP ratio. Participants involved in ATP buffering (according to the reference reactions) are underlined



(The actual proton turnover depends on pH and Mg^{2+} levels; cf. Ref. 23.)

The effect of each parameter on AK equilibrium was calculated as a shift from the unbuffered rate of ATP depletion toward maintenance of constant ATP levels with the assumption that the levels of the other participants were constant. The unbuffered rate of anaerobic ATP utilization results from the summed depletion of ATP and phosphagen levels as found experimentally. An iterative calculation procedure was used to determine at which ATP concentration the minimum value of ATP free energy change was reached, thus illustrating which minimum ATP concentration each parameter is able to buffer at the expense of the phosphagen.

Up to third-order polynomial regressions were calculated to depict the correlated changes in metabolic and acid-base status with increasing swimming speed (Sigmaplot, Jandel Scientific). Usually, those regressions were chosen that yielded the highest correlation coefficient. Significance of change was evaluated at the 5% probability level by the determination of

correlation coefficients and an F test after an analysis of variance (Sigmastat, Jandel Scientific). Values differing significantly from the norm (Pearson and Hartley's and Nalimov's test) were completely eliminated from the data set. Maximum changes were evaluated for those data found within the 95% confidence interval (Table 1).

RESULTS

The pH_i in the mantle tissue of *L. brevis* fell progressively when the concentrations of anaerobic metabolites started to rise above the critical swimming velocity of 1.5–2 mantle lengths/s (cf. Ref. 11). Intracellular PCO_2 rose moderately beyond the same swimming speed, and bicarbonate levels fell (Fig. 1). Intracellular PCO_2 rose by a factor of ~ 1.6 . The depiction of pH and PCO_2 in Fig. 2 emphasizes that the decrease in pH and the rise in PCO_2 are correlated. The pH -bicarbonate diagram can be used to estimate the origin of the observed acidosis. The nonbicarbonate buffer value of the mantle tissue was determined as 23.7 ± 5.1 (SD)

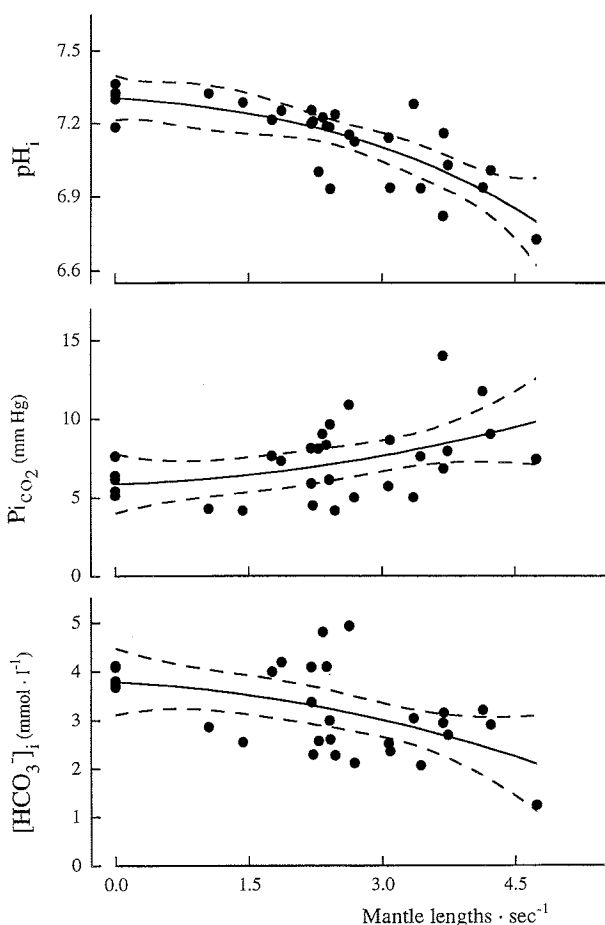


Fig. 1. Changes in intracellular acid-base parameters of mantle musculature in squid *Lolliguncula brevis* after swimming at different velocities. Solid lines were determined by regression analysis and delineate significant relationships ($P < 0.05$); dashed lines represent 95% confidence interval. pH_i , intracellular pH ($r = 0.77$, 3rd-order regression), Pi_{CO_2} , intracellular PCO_2 ($r = 0.45$, 2nd-order regression); $[\text{HCO}_3^-]_i$, intracellular apparent bicarbonate concentration ($[\text{HCO}_3^-]_i = C_{\text{CO}_2} - \alpha \cdot \text{PCO}_2$, where C_{CO_2} is tissue CO_2 concentration and α is the physical solubility of CO_2 in $\text{mmol} \cdot \text{l}^{-1} \cdot \text{mmHg}^{-1}$; cf. Fig. 2; $r = 0.51$, 2nd-order regression).

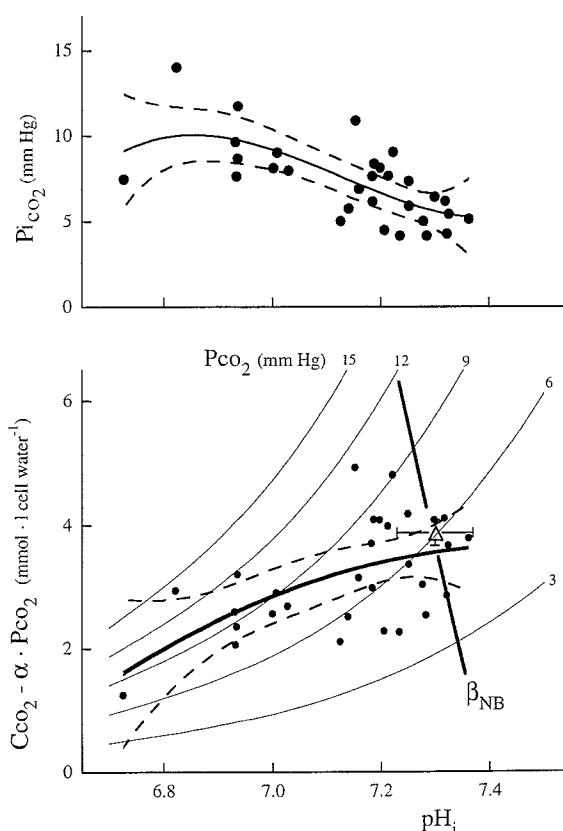


Fig. 2. Top: changes in Pi_{CO_2} with pH_i ($r = 0.69$, 3rd-order regression); bottom: changes in acid-base status of squid *L. brevis* mantle musculature displayed on a pH -bicarbonate diagram ($r = 0.56$, 2nd-order regression). Δ , Control values (means \pm SD). β_{NB} , Nonbicarbonate buffer line of muscle cell water. Solid lines were determined by regression analysis and delineate significant relationships ($P < 0.05$); dashed lines represent 95% confidence interval.

$\text{mmol} \cdot \text{pH unit}^{-1} \cdot \text{kg}^{-1}$ ($n = 6$), with the assumption of tissue free P_i levels of $1 \mu\text{mol/g}$ wet wt in accordance with previous ^{31}P -NMR investigations (Pörtner et al., unpublished observations). For use in the pH -bicarbonate diagram, this value was transformed to the equivalent value of $42.2 \text{ mmol} \cdot \text{pH unit}^{-1} \cdot \text{l cell water}^{-1}$. The pH -bicarbonate analysis demonstrates that respiratory and nonrespiratory processes are responsible for the development of a progressive and uncompensated intracellular acidosis, however, with a large predominance of nonrespiratory influences.

The contribution of anaerobic metabolism to the development of the acidosis is illustrated by the correlated changes in pH_i and octopine levels. The respective curve indicates a linear relationship in the range of high, but not low, octopine concentrations: At low octopine levels, pH_i fell to a larger extent without a similar rate of octopine accumulation as seen in the range of high octopine contents (Fig. 3, see Fig. 7). The progressive acidosis also played an important role in phosphagen breakdown, as suggested by the clear correlation between pH_i and the level of PLA. PLA depletion with falling pH_i was accompanied by a rise in L-Arg levels, which, however, was less than the fall in PLA, because part of the arginine was consumed in

octopine formation. After depletion of PLA at low pH_i , the pattern of correlation between arginine levels and pH_i reveals that continuing octopine formation progressively decreased the level of L-Arg.

The progressive drop in pH_i as it was associated with increased swimming velocities above the anaerobic threshold changes the dissociation equilibria of metabolic substrates (25). Figure 4 depicts the changes in the level of monohydrogenphosphate, the true substrate of glycogen phosphorylase. At constant phosphate concentrations, this level would be expected to decrease owing to the developing acidosis. However, the concomitant accumulation of P_i caused the level of monohydrogenphosphate to rise, despite falling pH_i . Monohydrogenphosphate levels reached a plateau at an elevated concentration when pH_i fell to values below ~ 7.15 . From a quantitative point of view, the metabolism of phosphate is one important process affecting the proton turnover during exercise (cf. Ref. 23). Proton uptake accompanies P_i release from the phosphagen

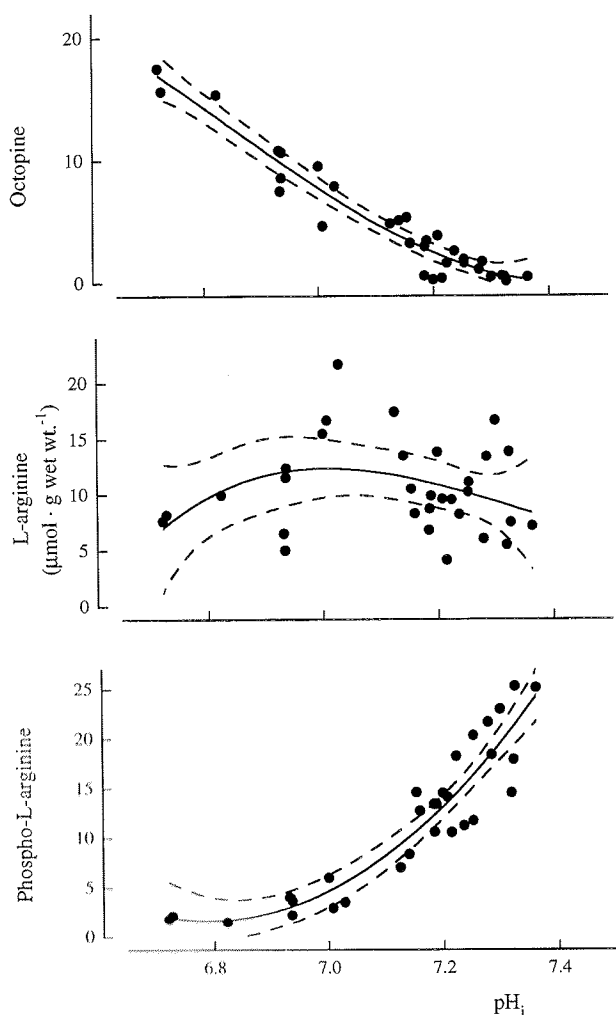


Fig. 3. Correlation between pH_i and metabolite levels in mantle tissue of squid *L. brevis* as analyzed for octopine ($r = 0.97$, 3rd-order regression), L-arginine ($r = 0.35$, 3rd-order regression), and phospho-L-arginine ($r = 0.93$, 3rd-order regression). Solid lines were determined by regression analysis and delineate significant relationships ($P < 0.05$); dashed lines represent 95% confidence interval.

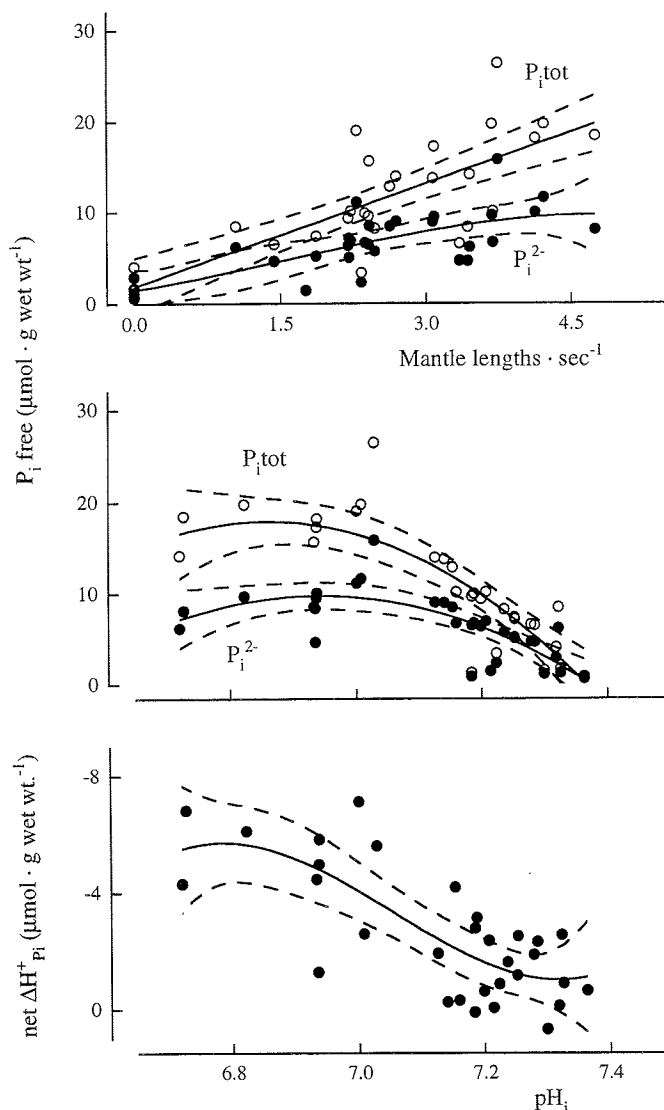


Fig. 4. Free monohydrogenphosphate levels (P_i^{2-}) and levels of free total P_i ($\text{P}_{i\text{tot}}$, calculated from data in Ref. 11) in mantle tissue of squid *L. brevis* after swimming at different velocities (top, normalized in mantle lengths/s; P_i^{2-} : $r = 0.74$, 3rd-order regression; $\text{P}_{i\text{tot}}$: $r = 0.79$, linear regression) and compared with changes in pH_i (middle, P_i^{2-} : $r = 0.74$, 2nd-order regression; $\text{P}_{i\text{tot}}$: $r = 0.82$, 2nd-order regression). Bottom: proton quantities (net $\Delta\text{H}^+_{\text{P}_i}$) bound by P_i during phosphagen hydrolysis (balanced to some extent by proton release during net phosphate release from MgATP; $r = 0.75$, 3rd-order regression, calculations valid for free $\text{Mg}^{2+} = 1$ mmol/l). Solid lines were determined by regression analysis and delineate significant relationships ($P < 0.05$); dashed lines represent 95% confidence interval.

via MgATP. Phosphate release during net depletion of MgATP and MgADP is associated with H^+ release. The change in net proton turnover by P_i (net $\Delta\text{H}^+_{\text{P}_i}$) is sigmoidal with an almost linear relationship over a wide range of pH (Fig. 4, bottom). The third-order regression indicates that proton uptake levels off at $\text{pH} \sim 6.8$.

The effective Gibbs free energy change of ATP hydrolysis in the mantle tissue fell linearly with rising swimming velocities starting at a mean value for controls of -56.8 ± 1.7 kJ/mol (Fig. 5). This control value may appear as a low estimate should PLA

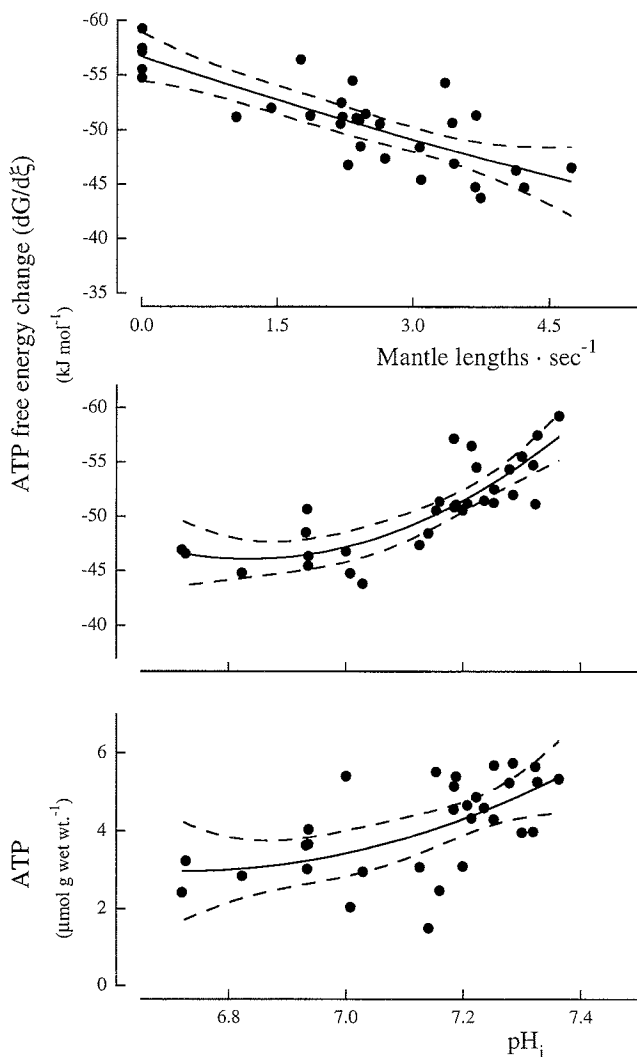


Fig. 5. Changes in effective Gibbs free energy change of ATP hydrolysis ($dG/d\xi$) in mantle tissue of squid *L. brevis* after swimming at different velocities (top, $r = 0.80$, 2nd-order regression) and as correlated with changes in pH_i (middle, $r = 0.83$, 2nd-order regression). Bottom: correlated decrease in pH_i and ATP levels ($r = 0.60$, 2nd-order regression, calculations valid for free $Mg^{2+} = 1$ mmol/l). Solid lines were determined by regression analysis and delineate significant relationships ($P < 0.05$); dashed lines represent 95% confidence interval.

hydrolysis to P_i and L-Arg be the source for the elevated free P_i that is typically (but not always) found during invasive analysis in control tissue samples. In this case, true levels would possibly approach -60 kJ/mol when most P_i is added to measured PLA levels, decreasing L-Arg concentrations by the respective amount. However, this is most unlikely, because a ratio of phosphagen to phosphagen + aphosphagen levels close to 0.7 appears typical for some, including vertebrate, muscle tissue, even when P_i levels are very low. The actual ratio will depend on pH_i and the level of free ADP, both of which may vary depending on the specific pattern of acid-base regulation and the metabolic rate of the tissue (21). Therefore, control values are likely to be only slightly underestimated owing to the effects of tissue sampling and extraction procedures, and ele-

vated levels of P_i possibly found in perchloric acid extracts must originate from sources like mitochondria (see MATERIALS AND METHODS).

The lowest value of the effective Gibbs free energy change of ATP hydrolysis reached at maximum speeds within the 95% confidence interval was found at -44.7 kJ/mol (Table 1). Figure 5 also shows that effective ATP free energy change levels "dropped" with falling pH_i initially but remained constant in a range of low pH_i (the term "drop" refers to the decrease in driving force, whereas the actual number rises from negative to more positive values). The fall in pH_i was also correlated with a progressive net decrease in ATP levels.

DISCUSSION

Most previous work on exercise-induced changes in muscle metabolism and acid-base status in vivo focused on a comparison of extremes between rest and fatigue. Previously data were compiled from squid *I. illecebrosus* reaching fatigue with variable contributions of anaerobic glycolysis and from animals recovering after fatigue (28, 31, 32). The progressive intracellular changes during the actual period of muscular work have mostly been investigated in humans or in isolated vertebrate or invertebrate muscle preparations by use of ^{31}P -NMR (5, 8, 34). The present data now allow an analysis of the progressive and interrelated changes in metabolism and acid-base status in the squid *L. brevis* in vivo during swimming at various submaximum and maximum speeds.

The methodology applied in the present study allows a delineation of transitional changes based on the depiction of individual data. It also permits an estimate of variability between individuals, as discussed in our previous study (11). Interestingly, the variability apparent in the metabolic responses to increasing swimming speeds is reduced when the correlated changes in pH_i and PCO_2 , as well as metabolite levels, are analyzed, supporting the accuracy of our analyses for individual squid and our previous conclusion that a rather large variability exists in the performance levels of individual squid in the same way as between individual human subjects (11).

Acid-base regulation. The pattern of changes observed in the intracellular acid-base status of *L. brevis* is similar to the pattern seen previously in *I. illecebrosus* during fatiguing exercise and recovery. The present data demonstrate, however, that a progressive respiratory and nonrespiratory acidosis starts to develop only above the critical swimming speed (Figs. 1 and 2), which according to our previous study (11) is defined as the swimming velocity above which an anaerobic metabolism sets in to contribute to energy production. This finding is similar to the onset of intracellular acidosis characterizing the anaerobic threshold in humans (20, 34). In the pH -bicarbonate diagram of Fig. 2, the bulk of the data points is scattered in the proximity of mean control values. The reason is that the development of progressive acidosis is observed only above the critical swimming speed. This is also confirmed by the correlated changes in pH_i and intracellular PCO_2 in Fig.

2. Intracellular PCO_2 in the mantle was high, especially when pH_i had reached low values above the critical swimming speed.

The factorial rise in intracellular PCO_2 at the highest swimming velocities (by ~ 1.6) is similar to the factorial rise in oxygen consumption during increased swimming. This finding suggests that the rise in energy requirements with increasing swimming speed (11) would be the reason for increased CO_2 production and elevated tissue intracellular PCO_2 . Overall, the factorial rise in oxygen consumption and the degree of respiratory acidification are small compared with the factorial changes in similarly active fish (22). The major impact on cellular acid-base status therefore arises from the progressive contribution of anaerobic metabolism.

Metabolic correlates of changes in pH_i . The biochemical assays at different activity levels allow the description of the correlated changes in pH_i and the levels of high-energy phosphates and other metabolites in vivo. The correlated changes in metabolic and acid-base parameters provide insight into the importance of acid-base parameters in metabolic regulation and vice versa.

Similar to our previous findings in *I. illecebrosus* (31), the relationship between octopine levels and pH_i was close to linear after an initial drop in pH_i (Fig. 3, see Fig. 7). Such a drop had been observed in *I. illecebrosus* and had been demonstrated to reflect an initial release of base equivalents into the blood from the mantle muscle with the onset of exercise. This base release was interpreted to protect oxygen transport by the respiratory blood pigment hemocyanin from extracellular respiratory acidification (28). Such a feature may be of general importance in exercising squid.

PLA levels fell almost linearly with pH until depletion was close to complete. Because PLA breakdown is mirrored by the release of P_i via ATP hydrolysis (see Eq. 13), phosphate accumulation also leveled off in a low range of pH (Fig. 4). The comparison of mean levels of organic phosphate and P_i in control and fatigued animals (Table 1 in Ref. 11) suggests that the P_i does not leave the muscle cells during fatigue.

The pH-octopine relationship can be interpreted as the effective in vivo buffer line for glycolytic protons. Figure 7 illustrates that it deviates from the nonbicarbonate buffer line and indicates a higher buffer value in vivo than expected from the nonbicarbonate buffer value under resting conditions. This deviation cannot be explained by the decrease in bicarbonate levels with progressive acidosis (Fig. 1). It will, however, reflect the rise in phosphate concentration, which increases the amount of nonbicarbonate buffers 1) by the concentration change itself and 2) by the rise in phosphate buffer value as pH falls to values close to the pK' of P_i . Consequently, phosphagen breakdown is the predominant buffering process, because it is linked to proton consumption depending on the actual value of pH_i . The stoichiometric proton uptake increases as pH falls (for more theoretical details see Ref. 23). Obviously, this process compensates to some extent for the exponential increase in phosphate levels with falling pH, turning

the rise in proton uptake with falling pH into a sigmoidal process (Fig. 4). However, it needs to be emphasized that not all the accumulating phosphate originates from the phosphagen. Some is released during net MgATP and MgADP degradation and is linked to net proton release. This process has been considered in Fig. 4 (bottom). The variability in the results of this analysis is introduced by the additive variability of phosphate and ATP levels between individual squid. Overall, the proton binding by accumulating phosphate offers the basis for a quantitative explanation of the discrepancy between effective and nonbicarbonate buffer lines (see Fig. 7). In *L. brevis* the discrepancy is somewhat less than in *I. illecebrosus* owing to less P_i accumulation in *L. brevis* and less P_i accumulation than expected from the analysis of phosphate proton binding (Fig. 4). The reason for this is additional proton production by other metabolism (i.e., in succinate formation, cf. Refs. 23 and 28), which reduces the net effect of proton binding by accumulating phosphate. The results of the respective analysis support the assumption that the levels of PLA, ADP, AMP, and pH are in or close to equilibrium owing to the action of myokinase and AK.

ATP free energy change: a causal factor in fatigue? Resting ATP free energy change was around -57 kJ/mol, which is somewhat lower than -60 kJ/mol found by Combs and Ellington (6) in isolated molluscan muscle at rest by use of ^{31}P -NMR or -64 kJ/mol in isolated sipunculid muscle by use of the present methodology (34). These comparisons suggest that the observed differences are not caused by use of invasive vs. noninvasive methodologies but, rather, reflect the functional status or the metabolic rate of the muscle under investigation. The lower resting values in squid are likely to be associated with the high baseline metabolic rate.

Apparently, the energy status of working mantle muscle remained more or less unchanged at a low level once pH fell to < 7.0 . That a fall in pH is detrimental for the energy status would appear as an obvious conclusion from the data in Fig. 5. However, it has to be considered that the term "ATP free energy change" is derived from various parameters, e.g., pH and concentrations of ATP, free ADP, P_i , and free Mg^{2+} . With the assumption of constant levels of all these parameters, pH by itself causes a drop in standard and in vivo ATP free energy change values by only ~ 2 kJ/mol with a minimum below pH 7.0 (27). In squid mantle, a minimum is reached at similar pH values, but a much larger change occurred that can only partly be caused by the acidosis and, rather, follows the depletion of ATP and the accumulation of ADP and P_i . Our previous work (32) suggested a minimum value for ATP free energy change, indicating the onset of contractile failure or fatigue generally and independent of pH. This conclusion is supported by the observation that the respective change in energy status was similar in fatigued *I. illecebrosus* and *L. pealei*, although pH fell by ~ 0.6 unit in *Illex* mantle but only by < 0.1 unit in *Loligo*. As a corollary, the drop in ATP free energy occurred to the

same extent in fatiguing muscle regardless of whether pH falls at the same time (cf. Table 1).

This conclusion remains speculative as long as the requirement of ATPases in terms of ATP free energy remains obscure. This requirement is likely to change depending on the turnover rate of ATPases, such that the coupling between function and available ATP free energy is not tight. Nonetheless, the minimum value of around -44 kJ/mol reached during fatigue in *L. brevis* is already below those calculated by Kammermeier (17, 18) as being required for the function of ATPases in rat myocardium (-49 , -51 , and -53 kJ/mol for sarcolemmal Na^+ - K^+ -ATPases, Ca^{2+} -ATPases, and sarcoplasmic reticulum Ca^{2+} -ATPase, respectively, and -45 – 50 kJ/mol for actomyosin-ATPase). Kammermeier's values are those required for steady-state function of those ATPases and not necessarily those reflecting the functional limit. This means that, in a sense of an elastic coupling of energy availability and demand, changes in ionic distribution equilibria in accordance with a decreased ATP free energy may be tolerated to some extent before cellular function is impaired. Moreover, Combs and Ellington (6) in preliminary calculations evaluated a steady-state energy requirement of approximately -41 kJ/mol for sarcolemmal Ca^{2+} -ATPase in *Mytilus edulis* anterior byssus retractor muscle. This value is below that for rat myocardium, suggesting differences between species and tissues. However, resting free energy values are similar in vertebrate and invertebrate groups, leaving the answer to this question open.

Previously, we discussed that the acidosis in *I. illecebrosus* protects ATP from being largely degraded (32). Down to the minimal value of ATP free energy change, more ATP was depleted in *L. pealei* and more ADP and AMP accumulated. Similar conclusions arise when the data from *L. brevis* are included in this comparison (Table 1). Quantitative analysis reveals that the fall in pH is caused quantitatively by mechanisms that are associated with substrate level phosphorylation (23, 24). Actually, substrate level phosphorylation requires (net or transient) proton release from the substrate (23). Therefore, an acidosis, although decreasing the actual value of the free energy change of ATP hydrolysis to some extent (see above; 6, 27), is in most cases associated with complementary ATP production, compensating for this apparent disadvantage and delaying the progressive depletion of ATP levels and the fatal decrease in ATP free energy change (for the additional role of the phosphagen see below). This conclusion is also supported by the fact that the free energy change value remained more or less unchanged when pH was <7.0 (Fig. 5), indicating that fatigue set in at similar free energy values in animals with a variable contribution of anaerobic glycolysis to ATP production and acidosis (cf. Table 1). Moreover, the ATP free energy change values found after fatigue in the mantle muscle of *I. illecebrosus* and *L. pealei* are the lowest so far reported in fatigued (mostly vertebrate) muscle tissue (cf. Ref. 12) and may represent an example where

fatigue is elicited by the reduction of available energy to essential ATPases.

Importance of free Mg^{2+} levels. Previously, Combs and Ellington (6) described a drop in free cellular Mg^{2+} levels to occur with falling pH, in a marine invertebrate muscle preparation. As also stated by these authors, such a drop would have a large effect on the standard free energy change, where values are 2.8 kJ/mol larger when free Mg^{2+} levels are 0.1 instead of 2 mmol/l. However, the importance of free Mg^{2+} levels for the free energy change of ATP hydrolysis in vivo is far less, because concentration ratios change considerably between standard and in vivo conditions. In our experiment the free energy change of ATP hydrolysis would shift to minimal values only 0.04 kJ/mol below the values depicted in Fig. 5 for exhausted animals should free Mg^{2+} fall from 1 to 0.1 mmol/l. Similarly, in a resting specimen the free energy change would amount to -56.9 kJ/mol at 2 mmol Mg^{2+} /l (above the in vivo concentration of free Mg^{2+}) and fall to only -56.7 kJ/mol should free Mg^{2+} levels fall to 0.01 mmol/l, a concentration below the in vivo levels. In conclusion, the effective in vivo free energy change of ATP hydrolysis is rather insensitive to fluctuations in free Mg^{2+} levels in resting as well as fatigued animals. These observations do not support a significant protective function of a decrease in free Mg^{2+} levels on ATP free energy change values suggested by Combs and Ellington (6). Nonetheless, the level of free Mg^{2+} in the cell is important for cellular function, because it determines the concentration of MgATP or MgADP, the only species used by kinases and ATPases (cf. Ref. 23). Should free Mg^{2+} levels fall from 1 to 0.1 mmol/l, this would cause a decrease in MgATP²⁻ and MgADP⁻ levels by 20 and 71% , respectively. This decrease in the concentration of functional adenylates (under more or less constant levels of ATP free energy) is the reason why, at some point, a falling Mg^{2+} concentration will become harmful for cellular energetics.

Role of the phosphagen. Phosphagen depletion buffers ATP levels. Nonetheless, it will, by an increase in phosphate levels, cause the free energy change of ATP hydrolysis to fall. If anaerobic glycolysis is involved, phosphagen depletion will, however, compensate for this apparent disadvantage by two processes: 1) by buffering the metabolic protons released in anaerobic glycolysis and slowing the pH decrease (23) (see Fig. 7) and 2) by causing a rise in the concentration of monohydrogenphosphate, the actual substrate of glycogen phosphorylation (cf. Ref. 25). Under conditions when the phosphate concentration remains constant, a decrease in pH would otherwise cause proton binding by P_i and, consequently, a drop in monohydrogenphosphate levels. Phosphagen depletion not only compensates for this decrease but causes an accumulation of monohydrogenphosphate, thus supporting glycogen breakdown. Actually, in vertebrate and some marine invertebrate muscles, phosphate accumulation is seen as one important factor activating glycogen breakdown (19). Our present analysis quantifies the concentration of this

true substrate of glycogen catabolism during progressive muscular exercise.

Buffering of both ATP levels and ATP free energy change values. Figure 6 models the buffering of ATP levels and ATP free energy change values by the transphosphorylation of the phosphagen PLA, inasmuch as it depends on each individual experimental parameter, the decrease in pH_i , the accumulation of free ADP, and the removal of arginine by octopine. Unbuffered ATP depletion calculated as being equivalent to the measured depletion of the sum of ATP and PLA levels would cause the ATP free energy change to fall early to the observed minimum and would not allow the animals to reach a swimming speed higher than critical. It becomes obvious that even the observed small changes in free ADP concentrations cause significant ATP buffering and an increase in the maximum swimming velocity, but the effect is less than the transphosphorylation caused by each, the formation of octopine, and, even more so, the fall in pH_i . This model also illustrates that the combined and integrated action of all mechanisms of ATP buffering finally allows the animals to exceed the critical swimming speed (1.5 mantle lengths/s) by a factor of ~ 3 .

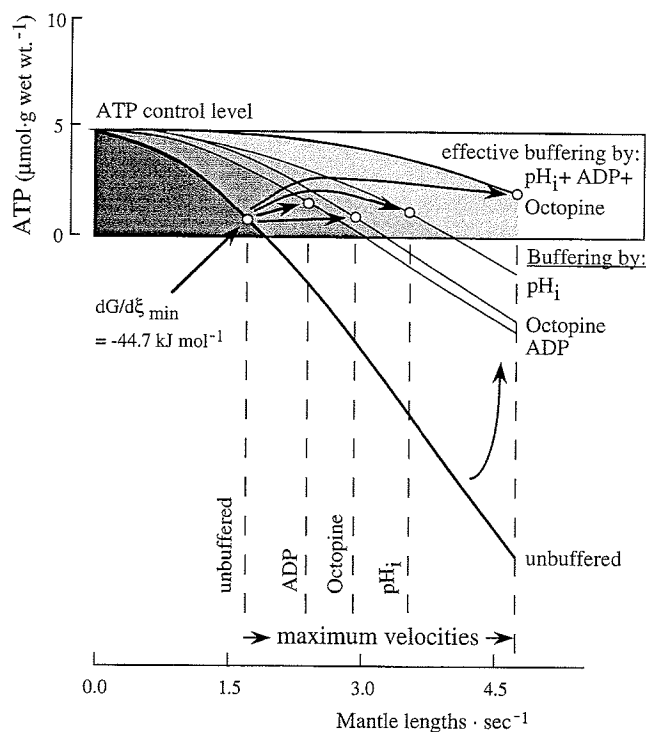


Fig. 6. Model effects of changes in pH_i and in concentrations of free ADP and octopine on buffering of ATP concentrations and of levels of Gibbs free energy change of ATP hydrolysis by transphosphorylation of phospho-L-arginine. Individual effect of each of measured parameters on arginine kinase reaction was calculated assuming that levels of other participants remained constant. Efficiency of buffer effect becomes evident with rightward shift of ATP depletion from unbuffered rate of ATP degradation during increased swimming. Unbuffered rate of ATP depletion was calculated as depletion of summed levels of ATP and phosphagen (calculations valid for free $Mg^{2+} = 1$ mmol/l). \circ , ATP concentration at which minimum level of effective Gibbs free energy change of ATP hydrolysis is reached. Shading shows improved buffering from left to right.

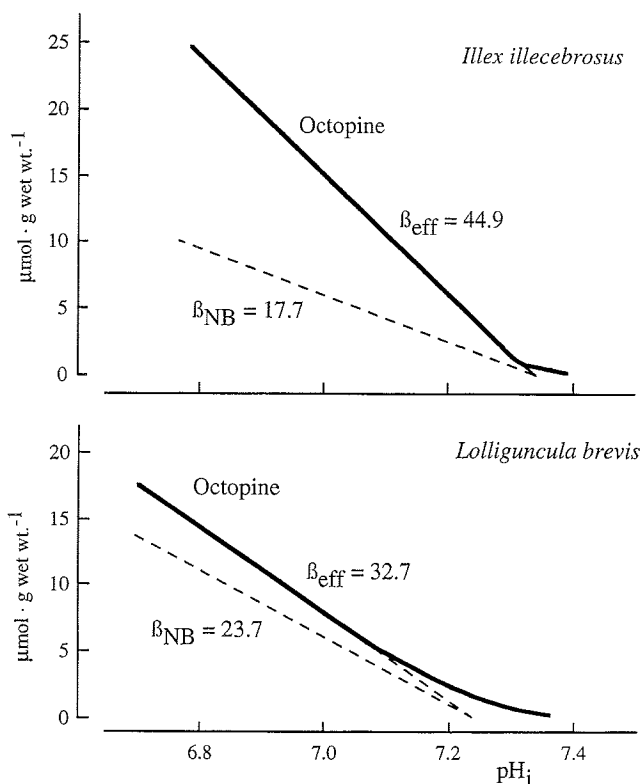


Fig. 7. Comparison of relationship between octopine levels and pH_i in mantle tissues of squids *L. brevis* and *Illex illecebrosus*. This relationship reflects effective buffer value of tissue (β_{eff}) for glycolytic protons and quantifies the extent to which glycolytic protons are buffered in vivo. Nonbicarbonate buffer lines (β_{NB}) determined in vitro (dashed lines) reflect physicochemical buffering starting from control pH_i values.

The model emphasizes to what extent buffering of ATP levels is linked to a buffering of ATP free energy change values that are decreased already by the accumulation of P_i associated with phosphagen depletion. Actually, this decrease can be considered advantageous, because the acidosis and the accumulation of P_i have some protective effect on ATP concentrations. P_i accumulates via ATP hydrolysis (Eq. 13), leading to a decrease in ATP free energy that is less, however, than that seen with unbuffered ATP depletion. In consequence, the minimum level of ATP free energy is reached at higher ATP contents with the use of the phosphagen than without (Fig. 6). Further comparative analyses are required to establish similar relationships in various animal groups and muscle tissues.

Strategies in shallow water environments. Although at first sight mantle tissues of the ommastrephid squid *I. illecebrosus* and the loliginid squid *L. brevis* appear similar in their metabolic response to swimming above the anaerobic threshold, differences become obvious when the relationships between octopine levels and pH_i are compared (Fig. 7). The slope of this relationship reflects the response of the tissue to glycolytic acidification in vivo, inasmuch as it results from intracellular physicochemical and metabolic buffering processes and proton-equivalent ion exchange between tissue and blood. The latter was found to be negligible in *I.*

illecebrosus (28). The comparison reveals that the slope of the in vivo titration curve (effective buffer line) is closer to the slope of the nonbicarbonate buffer line in *L. brevis* than in *I. illecebrosus*. Most of this difference between the two squid species will be explainable by different characteristics of phosphagen turnover in addition to a reduced amount of phosphagen available to *L. brevis*. Contrary to the situation in *L. brevis*, free ADP levels were less buffered in *I. illecebrosus* and *L. pealei* and rose considerably during fatiguing exercise, thus triggering PLA depletion to a larger extent than in *L. brevis* (Table 1). The lower buffering of glycolytic protons in *L. brevis* is due to this mechanism, because less P_i accumulates. Obviously, *L. brevis* utilizes acidification rather than the accumulation of free ADP to elicit phosphagen transphosphorylation and ATP buffering, whereas *L. pealei* mostly uses ADP accumulation and *I. illecebrosus* uses both, with the result of more effective metabolic proton buffering and protection of ATP levels than in *L. pealei*.

These differences reflect a delayed depletion of the phosphagen starting from lower concentrations and also less decrease in the Gibbs free energy change of ATP hydrolysis in *L. brevis* than in *Illex* and *Loligo*. Obviously, the common brief squid uses an economical strategy in the depletion of high-energy phosphates. This parallels to some extent the situation in the burrowing worm *Sipunculus nudus*, which also uses its large phosphagen stores, PLA, during extended time periods. It is able to prevent the level of ATP free energy change from falling below -49 kJ/mol, inasmuch as it may be required during extended digging excursions in the anoxic sediment (Pörtner, unpublished observations). A trend to reduce performance at higher levels of ATP free energy change might also be related to the extended period of anaerobic exercise in the brief squid (cf. Table 1). Fatigue or the inability to maintain maximum swimming speeds may then no longer be related to the drop in ATP free energy change but may mirror the reduction in muscular performance elicited by the combined effects of low pH and elevated P_i levels on muscular performance (cf. Ref. 12). Actually, the lower degree of proton buffering in *L. brevis* (Fig. 7) means that pH falls more rapidly in this species and may cause a decrease in performance before the energy status reaches a critical low level. In a further step of comparing the three squid species, less acidosis (as in *L. pealei*) poses a higher threat of ATP degradation, causing more severe and, possibly, longer-lasting symptoms of fatigue at low energy levels, whereas a severe acidosis at reduced rates of phosphagen depletion (as in *L. brevis*) reduces performance and may support the more economical and long-term use of anaerobic resources. Maximum anaerobic ATP and phosphagen turnover combined with glycolytic proton production (as in *I. illecebrosus*) use the advantages of acidosis (protection of ATP levels owing to maximum exploitation of the phosphagen) at maximum levels of performance until the critical level of acidosis or energy status may be reached.

Table 1. Changes in free energy change of ATP hydrolysis in mantle musculature of three squid species during fatigue

	<i>Illex illecebrosus</i>	<i>Loligo pealei</i>	<i>Lolliguncula brevis</i>
Δ pH _i	-0.6	>0.1	-0.36 (max. -0.57)
Δ PLA, μ mol/g wet wt	-31.2	-22.5	-16 (-18.8)
Δ P _i , μ mol/g wet wt	+32.8	+35.9	+15.2 (+18.7)
Δ ATP, μ mol/g wet wt	-2.3	-3.9	-1.8 (-2.5)
Δ ADP _{tot} , μ mol/g wet wt	+1.7	+2.4	+1.0 (+1.3)
Δ ADP _{free} , μ mol/g wet wt	+0.8	+1.4	+0.22 (+0.32)
Δ AMP _{tot} , μ mol/g wet wt	+0.7	+2.1	+0.55 (+0.66)
Δ AMP _{free} , μ mol/g wet wt	+0.3	+0.8	+0.05 (+0.10)
dG/dξ, kJ/mol			
Rest	-56.2	-55.8	-56.8
Fatigue	-42.3	-41.8	-46.9 (-44.7)
Δ	+13.9	+14.0	+9.9 (+12.0)

pH_i intracellular pH; PLA, phospho-L-arginine; dG/dξ, effective Gibbs free energy change of ATP hydrolysis. Data for *I. illecebrosus* and *L. pealei* represent maximum changes (recalculated from Ref. 32). Data for *L. brevis* represent mean changes in animals exercised to fatigue (cf. Ref. 11). Values in parentheses show maximum changes when only those data within 95% confidence interval of regression analyses were considered.

Conclusions and summary. The changes in muscular energetics and acid-base status observed in *L. brevis* compared with *I. illecebrosus* and *L. pealei* mantle musculature during progressive anaerobic swimming strongly suggest that *L. brevis* uses an economical strategy to exploit anaerobic resources once a critical swimming speed is surpassed (11). In contrast to the situation in *I. illecebrosus* and *L. pealei*, changes in the levels of free ADP during increased swimming velocities are small and may be well buffered, because they are far less than the changes in total ADP. This enables *L. brevis* to use the phosphagen for extended time periods. With the limited accumulation of free ADP, octopine formation and the associated decrease in pH_i become more important in supporting PLA depletion and buffering of ATP levels and allowing the squid to exceed the critical swimming speed both in terms of velocity and the time period during which higher speeds are maintained. The levels of accumulated P_i are about two times lower in *L. brevis* than in the other species (32). This limits the disturbing effect on myosin-ATPase (12) but, nonetheless, provides enough monohydrogenphosphate for glycogen phosphorylase to function. The conclusion that this species uses anaerobic energy stores in a more economical manner is also supported by the observations that the animals oscillate between low pressure jets and bursts of high pressure jets to support elevated swimming speeds and that the associated rise in aerobic metabolic rate caused by this energy-sparing mode of activity is also very moderate (11).

The decrease in the effective Gibbs free energy change of ATP hydrolysis is also delayed in *L. brevis* as

a consequence of the acidosis and the limited and delayed accumulation of P_i and free ADP. In addition, the two offshore squids reach somewhat lower levels of the ATP free energy change than *L. brevis*, levels that may then be crucial in mantle muscle fatigue, whereas the acidosis at lower rates of phosphagen utilization in *L. brevis* is related to a better protection of energy levels and may even allow the brief squid to continue performance at a lower-than-maximum level.

The excellent technical and logistic help by the staff of the Marine Biomedical Institute is gratefully acknowledged.

This study was supported by NATO travel grants, Deutsche Forschungsgemeinschaft Grant Po 278/4 to 7, and National Institutes of Health Grants RR-01024 and RR-04226.

Alfred-Wegener-Institute Publication No. 1136.

Present address of E. Finke: Institut für Biologiedidaktik der Justus-Liebig-Universität Giessen, Karl-Glöckner-Str. 21 c, D-35394 Giessen, Germany.

Address for reprint requests: H. O. Pörtner, Alfred-Wegener-Institut für Polar- und Meeresforschung, Biologie I/Ökophysiologie, Columbusstraße, D-27515 Bremerhaven, Germany (E-mail: hpoertner@awi-bremerhaven.de).

Received 12 December 1995; accepted in final form 20 April 1996.

REFERENCES

1. **Alberty, R. A.** Standard Gibbs free energy, enthalpy, and entropy changes as a function of pH and pMg for several reactions involving adenosine phosphates. *J. Biol. Chem.* 244: 3290–3302, 1969.
2. **Alberty, R. A.** Calculation of the standard Gibbs free energy, enthalpy, and entropy changes for the hydrolysis of ATP at 0, 25, 37 and 75. In: *Horizons of Bioenergetics*, edited by A. San Pietro. New York: Howard Gest, 1972, p. 135–147.
3. **Bergmeyer, H. U., J. Bergmeyer, and M. Grassl** (Editors). *Methods of Enzymatic Analyses* (3rd ed.). Weinheim, Germany: Verlag Chemie, 1983–1986.
4. **Brett, J. R.** The respiratory metabolism and swimming performance of young sockeye salmon. *J. Fish. Res. Bd. Can.* 21: 1183–1226, 1964.
5. **Chih, C. P., and W. R. Ellington.** Metabolic correlates of intracellular pH change during rapid contractile activity in a molluscan muscle. *J. Exp. Zool.* 236: 27–34, 1985.
6. **Combs, C. A., and W. R. Ellington.** Graded intracellular acidosis produces extensive and reversible reductions in the effective free energy change of ATP hydrolysis in a molluscan muscle. *J. Comp. Physiol.* 165: 203–212, 1995.
7. **Curtin, N. A., and R. C. Woledge.** Energy changes and muscular contraction. *Physiol. Rev.* 58: 690–761, 1978.
8. **Dawson, M. J., D. G. Gadian, and D. R. Wilkie.** Muscular fatigue investigated by phosphorus nuclear magnetic resonance. *Nature Lond.* 274: 861–866, 1978.
9. **Doumen, C., and W. R. Ellington.** Intracellular free magnesium in the muscle of an osmoconforming marine invertebrate: measurement and effect of metabolic and acid-base perturbations. *J. Exp. Zool.* 261: 394–405, 1992.
10. **Ellington, W. R.** Phosphocreatine represents a thermodynamic and functional improvement over other muscle phosphagens. *J. Exp. Biol.* 143: 177–194, 1989.
11. **Finke, E., H. O. Pörtner, P. G. Lee, and D. M. Webber.** Squid life in shallow waters: oxygen limitation of metabolism and performance in exercising gulf squid, *Lolliguncula brevis*. *J. Exp. Biol.* 199: 911–921, 1996.
12. **Fitts, R. H.** Cellular mechanisms of muscle fatigue. *Physiol. Rev.* 74: 49–94, 1994.
13. **Goldberg, R. N., and Y. B. Tewari.** Thermodynamics of the disproportionation of adenosine 5'-diphosphate to adenosine 5'-triphosphate and adenosine 5'-monophosphate. I. Equilibrium model. *Biophys. Chem.* 40: 241–261, 1991.
14. **Grieshaber, M., E. Kronig, and R. Koormann.** A photometric estimation of phospho-L-arginine, arginine and octopine using homogeneous octopine dehydrogenase isoenzyme 2 from the squid, *Loligo vulgaris* Lam. *Hoppe-Seyler's Z. Physiol. Chem.* 359: 133–136, 1978.
15. **Gwynn, R. W., and R. L. Veech.** The equilibrium constants of the adenosine triphosphate hydrolysis and the adenosine triphosphate-citrate lyase reactions. *J. Biol. Chem.* 248: 6966–6972, 1973.
16. **Heisler, N.** Buffering and transmembrane ion transfer processes. In: *Acid-Base Regulation in Animals*, edited by N. Heisler. Amsterdam: Elsevier, 1986, p. 309–356.
17. **Kammermeier, H.** High energy phosphate of the myocardium: concentration versus free energy change. *Basic Res. Cardiol.* 82, Suppl. 2: 31–36, 1987.
18. **Kammermeier, H.** Efficiency of energy conversion from metabolic substrates to ATP and mechanical and chemiosmotic energy. *Basic Res. Cardiol.* 88: 15–20, 1993.
19. **Kamp, G.** Intracellular reactions controlling environmental anaerobiosis in the marine annelid *Arenicola marina*, a fresh look at old pathways. In: *Surviving Hypoxia: Mechanisms of Control and Adaptation*, edited by P. W. Hochachka, P. L. Lutz, T. Sick, M. Rosenthal, and G. van den Thillart. Boca Raton, FL: CRC, 1993, p. 5–17.
20. **Marsh, G. D., D. H. Paterson, R. T. Thompson, and A. A. Driedger.** Coincident thresholds in intracellular phosphorylation potential and pH during progressive exercise. *J. Appl. Physiol.* 71: 1076–1081, 1991.
21. **Meyer, R. A., G. R. Adams, M. J. Fisher, P. F. Dillon, J. M. Krisand, T. R. Brown, and M. J. Kushmerick.** Effect of decreased pH on force and phosphocreatine in mammalian skeletal muscle. *Can. J. Physiol. Pharmacol.* 69: 305–310, 1991.
22. **O'Dor, R. K., and D. M. Webber.** The constraints on cephalopods: why squid aren't fish. *Can. J. Zool.* 64: 1591–1605, 1986.
23. **Pörtner, H. O.** Contributions of anaerobic metabolism to pH regulation in animal tissues: theory. *J. Exp. Biol.* 131: 69–87, 1987.
24. **Pörtner, H. O.** Anaerobic metabolism and changes in acid-base status: quantitative interrelationships and pH regulation in the marine worm *Sipunculus nudus*. *J. Exp. Biol.* 131: 89–105, 1987.
25. **Pörtner, H. O.** The importance of metabolism in acid-base regulation and acid-base methodology. *Can. J. Zool.* 67: 3005–3017, 1989.
26. **Pörtner, H. O.** Determination of intracellular buffer values after metabolic inhibition by fluoride and nitrilotriacetic acid. *Respir. Physiol.* 81: 275–288, 1990.
27. **Pörtner, H. O.** Multicompartmental analyses of acid-base and metabolic homeostasis during anaerobiosis: invertebrate and lower vertebrate examples. In: *Surviving Hypoxia: Mechanisms of Control and Adaptation*, edited by P. W. Hochachka, P. L. Lutz, T. Sick, M. Rosenthal, and G. van den Thillart. Boca Raton, FL: CRC, 1993, p. 139–156.
28. **Pörtner, H. O.** Coordination of metabolism, acid-base regulation, and haemocyanin function in cephalopods. In: *Physiology of Cephalopod Molluscs—Lifestyle and Performance Adaptations*, edited by H. O. Pörtner, R. K. O'Dor, and D. MacMillan. Basel: Gordon and Breach, 1994, p. 131–148.
29. **Pörtner, H. O., R. G. Boutilier, Y. Tang, and D. P. Toews.** Determination of intracellular pH and PCO_2 after metabolic inhibition by fluoride and nitrilotriacetic acid. *Respir. Physiol.* 81: 255–274, 1990.
30. **Pörtner, H. O., N. Heisler, and M. K. Grieshaber.** Anaerobiosis and acid-base status in marine invertebrates: a theoretical analysis of proton generation by anaerobic metabolism. *J. Comp. Physiol. B Biochem. Syst. Environ. Physiol.* 155: 1–12, 1984.
31. **Pörtner, H. O., D. M. Webber, R. G. Boutilier, and R. K. O'Dor.** Acid-base regulation in exercising squid (*Illex illecebrosus*, *Loligo pealei*). *Am. J. Physiol.* 261 (Regulatory Integrative Comp. Physiol. 30): R239–R246, 1991.
32. **Pörtner, H. O., D. M. Webber, R. K. O'Dor, and R. G. Boutilier.** Metabolism and energetics in squid (*Illex illecebrosus*,

- Loligo pealei*) during muscular fatigue and recovery. *Am. J. Physiol.* 265 (Regulatory Integrative Comp. Physiol. 34): R157–R165, 1993.
33. **Reipschläger, A., and H. O. Pörtner.** Metabolic depression during environmental hypercapnia: the role of extra- versus intracellular pH in *Sipunculus nudus*. *J. Exp. Biol.* 199: 1801–1807, 1996.
34. **System, D. M., D. J. Kanarek, S. J. Kohlers, and H. Kazemi.** ³¹P nuclear magnetic resonance spectroscopy study of the anaerobic threshold in humans. *J. Appl. Physiol.* 68: 2060–2066, 1990.
35. **Teague, W. E., and G. P. Dobson.** Effect of temperature on the creatine kinase equilibrium. *J. Biol. Chem.* 267: 14084–14093, 1992.
36. **Tewari, Y. B., R. N. Goldberg, and J. V. Advani.** Thermodynamics of the disproportionation of adenosine 5'-diphosphate to adenosine 5'-triphosphate and adenosine 5'-monophosphate. II. Experimental data. *Biophys. Chem.* 40: 263–276, 1991.
37. **Vecchione, M.** Dissolved oxygen and the distribution of the euryhaline squid *Lolliguncula brevis* (Abstract). *Bull. Mar. Sci.* 49: 668–669, 1991.
38. **Veech, R. L., J. W. R. Lawson, N. W. Cornell, and H. A. Krebs.** Cytosolic phosphorylation potential. *J. Biol. Chem.* 254: 6538–6537, 1979.
39. **Wells, M. J.** The evolution of a racing snail. In: *Physiology of Cephalopod Molluscs—Lifestyle and Performance Adaptations*, edited by H. O. Pörtner, R. K. O'Dor, and D. MacMillan. Basel: Gordon and Breach, 1994, p. 1–12.
40. **Wolledge, R. C.** In vitro calorimetric studies relating to the interpretation of muscle heat experiments. *Cold Spring Harbor Symp.* 37: 629–634, 1978.

